

VERIFICATION OF THE IN-HOUSE DEVELOPED SIMULATOR SOFTWARE FOR COMMUNICATION SATELLITES

Anıl A. Aksu and Hilmi Sundu

Tübitak Space Technologies Research Institute, Çankaya, Ankara, Turkey, 06800

ABSTRACT

During the mission in orbit around the Earth, spacecraft get exposed to several sources of thermal loads which can be classified as external and internal. The external heat loads include solar flux, albedo flux, and the Earth IR radiation depending on orbital parameters whereas the internal loads are the heat dissipation caused by the electrical and mechanical inefficiency of equipment composing the spacecraft during its mission.

Even though the spacecraft gets exposed to periodic heating, the temperature of the spacecraft equipment have to stay within certain temperature limits. Regarding a communication satellite in geostationary orbit, while payload and external equipment would cool via the thermal radiation, temperature limits should be set within appropriate conduction and radiation links including the assistance of active heaters. The physical process and the configuration described above needs to be introduced appropriately to the computer to get a reasonable estimate of the temperature variation during the thermal cycle in the orbit. The physical model includes a continuous satellite components and the discrete radiation connection between them. The discretization of the physical processes, conduction, and radiation, leads to two separate thermal connectivity matrices. The non-linearity radiative heat transfer mode must be linearized around the temperature distribution vector which represents the temperature at each node of the discretized satellite. Furthermore, because of the non-linearity, most of the explicit time integration schemes are unstable. Therefore this type of problem requires implicit time integration method.

In the present study, Crank-Nicholson algorithm is preferred. It takes information from both the next time step and the current time step. It both increases the accuracy and the stability of the time integration. The implicit part of the time integration is also a root finding problem in higher dimensions. It is solved via multi-dimensional Newton-Raphson algorithm (Ober, 2004; Bates, 2001). Additionally, time step selection also plays an important role in both accuracy and more importantly stability. Differing from linear problems, a stable time step should be determined for every time step because of non-linear radiative heat transfer.

In this study, an in-house thermal code is developed for satellite simulator for simulating the thermal behavior of the spacecraft. The model is set on a newly developed communication satellite thermal mathematical model. Although the thermal model of the satellite would be

verified after thermal balance tests, the simulator aims to obtain same temperatures of the ones acquired by commercial software within temperature margins.

INTRODUCTION

In the last century, satellites played an important role in communication and earth observations. They are remotely controlled from ground stations. These stations retrieve various types of data from satellites (Kreng, 2005). In addition, autonomous on board computers (OBC) also serve both to control satellites and to perform the relevant data processing such as image processing (Guo-dong, 2009). Moreover, these on board computers can also simulate the physical processes such as heat transfer, electrical dissipation.

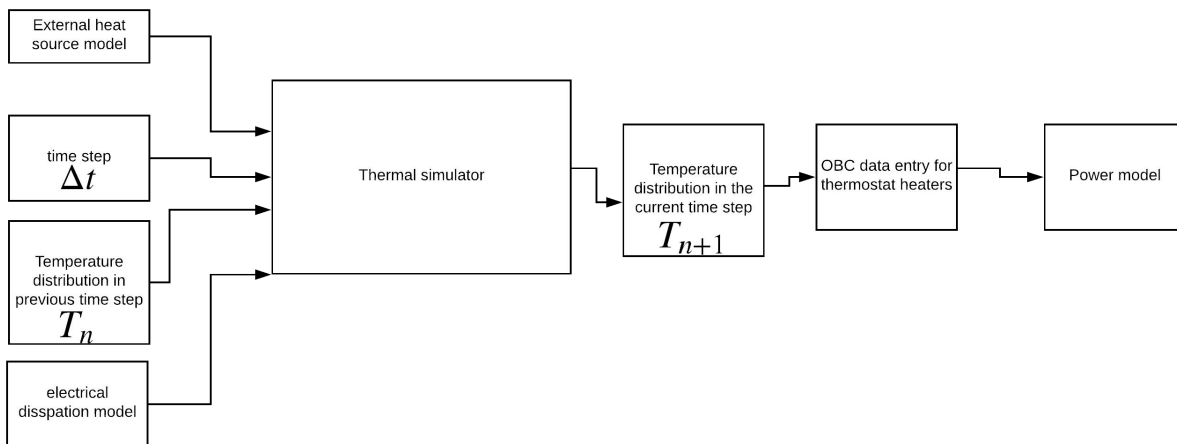


Figure 1: Thermal simulator input output diagram and its connection with the other parts of the total satellite simulator.

In general, these physical processes are analyzed by mathematically and numerically representing the associated physical problem. Similarly, these physical models can be introduced to the satellite's simulator to properly estimate the required physical results such as the temperature of the components, energy consumption and the trajectory of the satellite.

In this particular study, we are dealing with the thermal part of the simulator which is interconnected with the other parts of the simulator as shown in Figure 1. The thermal simulator takes inputs from electrical dissipation model and the other models that contribute to heating or cooling of the satellite and provides output to the whole simulator to control the heaters. Even though the satellite gets exposed to cyclic heating and cooling described above, the temperature of the satellite has to be held within certain limits. During the eclipse period, it needs to be heated whereas when it gets exposed to Sun beams directly, it needs to be cooled to protect the electronic devices inside the satellite body. The determination of the location

and the power of these heating and cooling instruments can be done after analyzing this thermal cycle and the heat flux distribution within the satellite. A simulation of the setting described above can be done before the design of satellite. Additionally, it would give a feedback to control system of cooling and heating system of a satellite dynamically (Richmond, 2010).

In the particular application, telecommunication satellites are considered. They are commonly orbiting outside the atmosphere (Gilmore, 2002). As a result, they are not affected by the atmospheric conditions and heat exchange with atmosphere via convection. The heat transfer modes included in the thermal simulator are conduction and radiation which enables to exchange thermal energy with Sun, Earth and outer space which is usually assumed to have $4K$ temperature. Not just radiation heat sources' presence, but also the location and the orientation of the satellite affects the amount of radiation heat flux into the satellite.

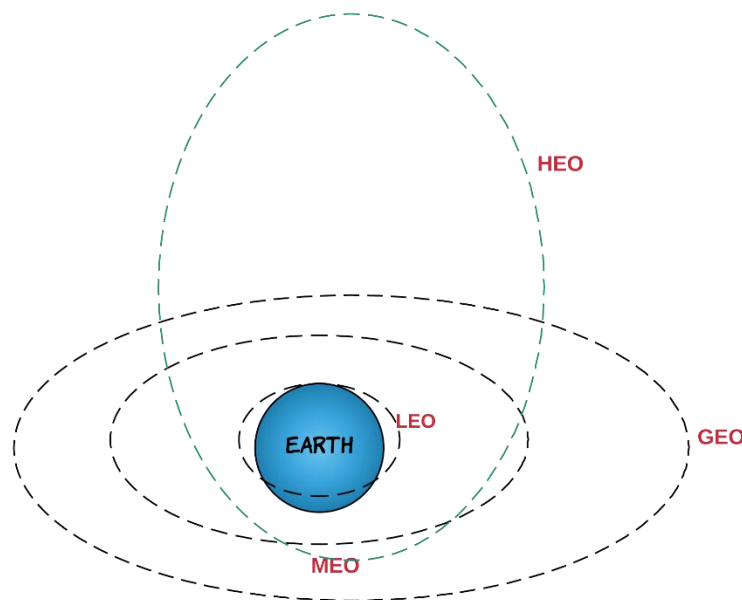


Figure 2: Schematic illustration of the common orbits.

The orbit type also determines the significance of the heat flow into satellite in terms of solar flux, albedo flux and IR flux. Most commonly preferred orbits can be listed as:

- GEO (Geo-stationary earth orbit)
- MEO (medium earth orbit)
- LEO (Low earth orbit)
- HEO (Highly elliptical orbit)

In detail, satellites in GEO have almost a distance of 36,000 km to the earth (O. Montenbruck, 2005; Gilmore, 2002) . For instance, all radio and TV, whether satellite etc, are launched in this orbit. There are several advantages satellites in GEO. Firstly, It is possible to cover almost all parts of the earth with just 3 geo satellites. Secondly, Antennas need not be adjusted every now and then but can be fixed permanently. Thirdly, The life-time of a GEO satellite is quite high usually around 15 years (O. Montenbruck, 2005; Gilmore, 2002) . Moreover, Satellite in MEO orbit operates at about 5000 to 12000 km away from the earth's surface (O. Montenbruck, 2005; Gilmore, 2002) . These orbits have moderate number of satellites and also simple in design. Compared with LEO system, MEO requires only dozen satellites.

Table 1: Properties of the most common orbit types

Parameter	LEO	MEO	GEO
Satellite Height	500-1500 km	5000-12000 km	35,800 km
Orbital Period	10-40 minutes	2-8 hours	24 hours
Number Of Satellites	40-80	8-20	3
Satellite Life	Short	Long	Long

In LEO satellites operate at a distance of about 500-1500 km. These satellite located in LEO orbit have some advantages and disadvantages. First of all, If global coverage is required, it requires at least 50-200 satellites in this orbit. Secondly, Special handover mechanisms are required and these satellites involve complex design. Thirdly, These satellite have very short life (Time of 5-8 years) Assuming 48 satellites with a life-time of 8 years each, a new satellite is needed every 2 months. In HEO orbit is made for satellites that do not revolve in circular orbits, only a very few satellite are operating in this orbit. Depending on the application and the satellite type, different type of orbit can be preferred.

During one full cycle around a orbit, net heat flux into a satellite dynamically changes. In eclipse, the earth obstructs the sun so that it disables satellite's view, therefore the satellite loses heat via radiation heat transfer. When it gets out of eclipse, it gets exposed to radiative heat flux directly and it starts heating the satellite. Moreover, it also gets exposed to heat flux due to sun beam's reflection from atmosphere so-called albedo (Pisacane, 2016) . However, its effect may become negligible depending on the proximity of the satellite to the earth. Similarly, Infrared radiation from the earth is also dependent on the distance between the earth and the satellite.

As a result, solar flux is effective in every type of orbit shown in Figure 2, however their albedo and IR heat fluxes are only effective in LEO and MEO orbits and their thermal

effect is variable in HEO. Detailed information about LEO, MEO and GEO orbits' thermal effects are given in Table 2. The orbit types also has its own challenge in terms of the global navigation systems (Capuano, 2013), however it is beyond the scope of this work.

Table 2: Thermal effects of different types of orbits

Types of Orbits	Space Thermal Environment Factors			
	Solar Radiaton	Albedo (Earth-Reflected Solar Flux)	Earth Infrared Radiation (IR Earth)	Aerodynamic Heating (Rarefied Gas)
LEO	Efective Solar Flux (1326–1417 W/m^2)	Efective (Strongly latitude – dependent)	Efective (At255K around 240 W/m^2)	P <10 ⁻⁵ Torr Not taken into account>300km
MEO	Efective	Efective	Efective	Neglegible
GEO	Efective Solar Flux (1326–1417 W/m^2)	Neglegible	Neglegible	Neglegible

The origin of the motivation of the present study is to model the heat transfer problem of the communication satellites realistically to protect it from excessive temperature variations which may become detrimental to the satellite in terms of fatigue of the electronic components (Sharon, 2015) by controlling the heaters in various locations of the satellite. The physical process and the configuration described above needs to be introduced appropriately to computer to get reasonable estimate of thermal cycle in the satellite.

Finally, the objectives of this study can be listed as deriving a discrete thermal model of a satellite and performing stable time integration. By doing so, a sufficient framework for a real time thermal satellite simulator is provided. Moreover, the discrete time integration part can also be used separately if a discrete thermal model is imported. In this present study, finite volume type discretization, where each element of discretization is treated as a control volume in terms of heat flow, is preferred similar to (Okan, 2002), however in simpler solution domains with

regular geometry like sphere or solid block, other researchers also formulated the radiative heat transfer with finite element formulation (Badri, 2018). The heat flux is distributed within the satellite through both radiation and conduction. A radiation link enables to transfer heat between components which are satellite's body, solar panels and reflectors. On the other hand, this net heat flux into satellite is also diffused in each component of the satellite via conductive heat transfer. The conductive heat transfer between the components of the satellite is negligible as the net area connecting the components are relatively small and the radiative heat exchange between them is more effective.

NUMERICAL ANALYSIS METHOD

The physical model includes a continuous satellite components and discrete radiative connection between them. First, each component has to be discretized appropriately. After discretizing components of the satellite, heat transfer modes can also be represented discretely (Kim, 2017; Okan, 2002). The discretization of the physical processes, conduction and radiation, leads to two separate thermal connectivity matrices.

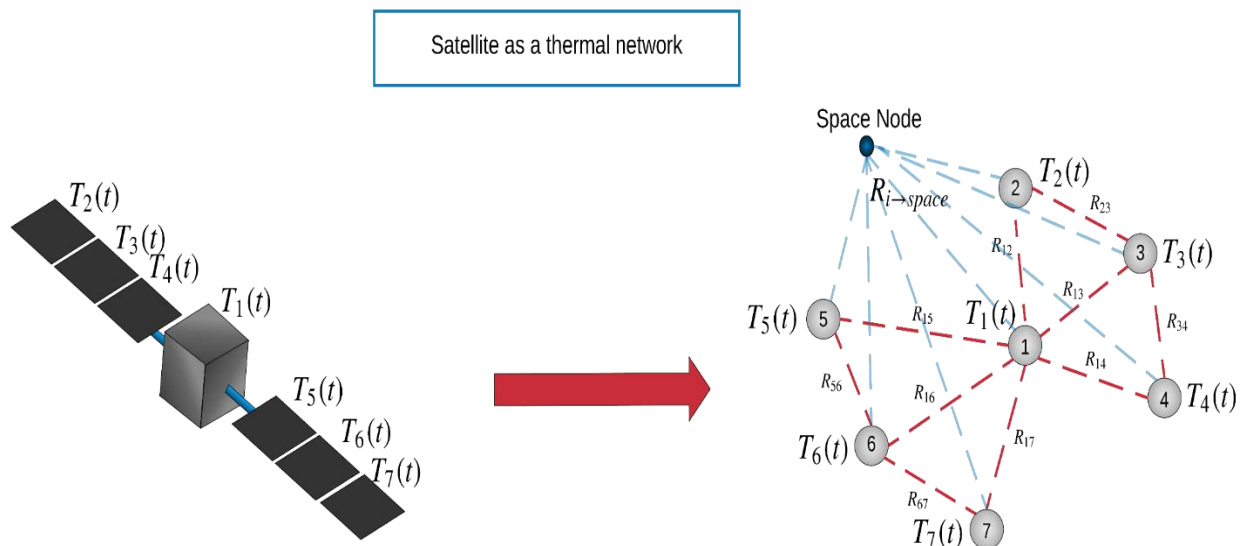


Figure 3: Sample satellite as a thermal network

After defining conductive connectivity and radiative connectivity matrices, all components of the satellite can be included in a single system simultaneously. Even though these components are not connected via conductive connectivity matrix, they are connected via radiative connectivity matrix. After discretization, both radiation and conduction can be written in discrete form (Okan, 2002). Discrete form of conduction can be written in terms of thermal conductance. The thermal conductance between each node can be given as:

$$K_{ij} = \kappa \frac{A_{ij}}{L_{ij}}$$

where A_{ij} is the effective area and L_{ij} is the distance between each diffusive node. As given by (Okan, 2002), the overall system can be discretely given as:

$$mc_{p_i} \frac{dT_i}{dt} = K_{ij}(T_j - T_i) + R_{ij}(T_j^4 - T_i^4) + F_i$$

Where mc_{p_i} is the thermal mass of the component denoted by i subscript. The equation above can also be given in the matrix notation as:

$$[M] \frac{d\vec{T}}{dt} = [K]\vec{T} + [R]\vec{T}^4 + \vec{F}$$

where $[M]$ is the thermal mass matrix which is formed by thermal mass of each node mc_{p_i} , $[K]$ is the conduction matrix, $[R]$ is the radiation matrix. The main focus of the work here is on both These connectivity matrices and the discretized satellite nodes form a non-linear thermal network problem. The total heat flux into each component is the sum of solar flux, albedo flux and Infrared flux (IR) and electrical dissipation due to electrical equipment. Moreover, it loses heat due to radiation to outer space, As a result, the external heat input can be given as:

$$F_i = F_i^{solar} + F_i^{albedo} + F_i^{IR} - F_i^{radiation} + F_i^{dissipation}$$

where F_i^{solar} is the solar heat flow, F_i^{albedo} is albedo heat flow and F_i^{IR} is the IR heat flow into i th component. Furthermore, $F_i^{dissipation}$ is volumetric heating in each component due to electrical dissipation and $F_i^{radiation}$ is radiative heat flow from i th component to the outer space.

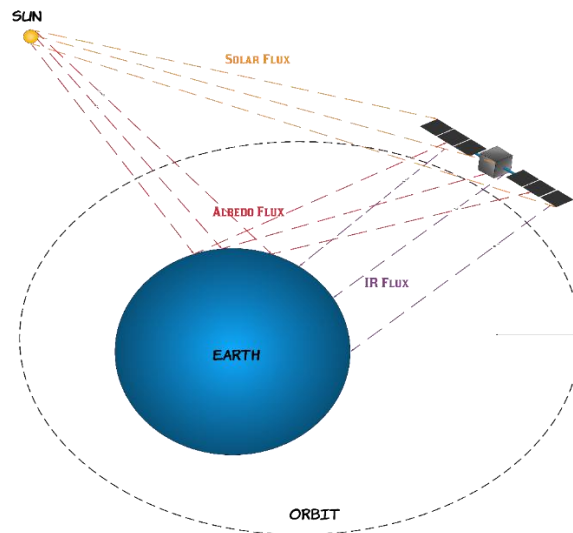


Figure 4: The schematic representation of the heat flux onto satellites.

Even if the problem is correctly formulated, numerical solution of the non-linear system is also not a straightforward time integration. The non-linearity radiative heat transfer mode must be

linearised around the temperature distribution vector which represents the temperature at each node of discretized satellite. It is done by writing the Jacobian matrix of the radiative heat transfer term which is the multiplication of $[K]$ with the forth power of the nodal temperature.

View factor computation

A radiation link between each node is established which is dependent on several factors like view factor emissivity ϵ , absorptivity α , reflectivity ρ and the surface area A_i . In calculations, the rule of reciprocity also plays key role:

$$F_{ij}A_j = F_{ji}A_i.$$

It basically says how much each surface sees each other is equal to each other. Moreover, even though a radiation link can be established between surfaces which can't see each other through other surfaces. Commonly these factors are computed via statistical approach such as Monte Carlo methods (Vujičić, 2006). In the particular application here, the view factors are calculated by a commercial software. In addition to the view factor computation, emissivity and Stefan-Boltzmann constant also multiplied with the forth power of the temperature of the each component to get the radiative heat flux between two nodes which can be given as:

$$Q_{i \rightarrow j} = \sigma F_{ji} A_i \epsilon (T_j^4 - T_i^4).$$

Under this formulation, the radiative connectivity matrix is defined as:

$$R_{ij} = \sigma F_{ji} A_i \epsilon.$$

Time Integration

Furthermore, because of the non-linearity, most of the explicit time integration schemes are unstable, therefore this type of problem requires implicit time integration method. In the present study, implicit algorithm is preferred. It takes information from both next time step and the current time step. It both increases the accuracy and the stability of the time integration compared to Euler and Runge-Kutta forth order (Chapra, 2006; Bates, 2001). Review of various time integration schemes are analyzed by (Ober, 2004). This type time integrators are called implicit. The implicit part of the time integration is also a root finding problem in higher dimensions. It is solved via multi-dimensional Newton-Raphson algorithm (Bates, 2001). Additionally, time step selection also plays an important role on both accuracy and more importantly stability which is also presented in present study. Differing from linear problems, a stable time step should be determined for every time step because of non-linear radiative heat transfer. As stated earlier, implicit time integration is employed for accuracy. Considering these issues, discrete model including radiative and conductive heat transfer mode can be given as:

$$[M] \frac{\vec{T}^{n+1} - \vec{T}^n}{\Delta t} = [K](\vec{T}^{n+1}) + [R](\vec{T}^{n+1})^4 + \vec{F}^n$$

where \vec{T}^n is the temperature distribution vector and \vec{F}^n is the total heat flow vector on time step n . It is implicit time integration formulation. Its numerical implementation requires a root

finding algorithm in higher dimensions. Even though root finding may seem to increase the complexity, as an initial guess to root finding at each time step, the current time steps' nodal temperature distribution can be taken, it significantly reduces the number of iterations to converge to the temperature distribution in next time step.

Root finding via Newton-Raphson in higher dimensions

The implicit formulation of the time integration takes information from the current time step and the next time step. The information from the current time step is taken explicitly which is not computationally expensive. However, implicit part of the time integration requires a root finding algorithm in multiple dimensions to proceed but it increase both the accuracy and the stability of the time integration. This problem can also be formulated as:

$$([I] - \Delta t[M]^{-1}[K])\bar{T}^{n+1} + \Delta t[M]^{-1}[R](\bar{T}^{n+1})^4 = \bar{T}^n + \Delta t[M]^{-1}\bar{F}^n$$

In further steps, the well-known Newton-Raphson iteration in higher dimensions is used. It is performed at each time step. Similar type of time integration approach for the radiation problem is also taken by (Bates, 2001). Explicitly, the new function is defined to take advantage of the Newton-Raphson iteration in higher dimension as:

$$\bar{G}(\bar{T}^{n+1}) = ([I] - \Delta t[M]^{-1}[K])\bar{T}^{n+1} + \Delta t[M]^{-1}[R](\bar{T}^{n+1})^4 - \bar{T}^n - \Delta t[M]^{-1}\bar{F}^n.$$

With the procedure described below, the root of $\bar{G}(\bar{T}^{n+1}) = 0$ is found. In higher dimensions, the Newton-Raphson iteration requires the computation of The Jacobian matrices of $\bar{G}(\bar{T}^{n+1})$ which is shown as $[J(\bar{T}_m^{n+1})]^{-1}$. Finally, the iteration can be given as:

$$\bar{T}_{m+1}^{n+1} = \bar{T}_m^{n+1} - [J(\bar{T}_m^{n+1})]^{-1}\bar{G}(\bar{T}_m^{n+1})$$

where the new subscript m is introduced to take the iteration into consideration, it is different than the time superscript n , it stands for the number of iteration. The objective of the formulation above is to find the temperature distribution minimizes L_{inf} of $\bar{G}(\bar{T}^{n+1})$.

RESULTS

Test Cases:

1-D Radiation problem

The most unstable part of the time integration is the non-linear term due to radiation. Its accuracy should be tested in a simpler setting before checking it in more realistic configuration. The analytical solution to the radiative heat transfer problem can only be solved under 1-D lumped mass assumption. The validity of lumped mass assumption in the convection problem can be determined by checking *Biot* number Bi which is basically the ratio between internal heat transfer resistance to the external heat transfer resistance (Çengel, 2003). For

sake of simplicity, in 1-D problem, It is assumed that $Bi \gg 1$ where the lumped mass assumption is valid, therefore the transient radiative heat equation can be given as:

$$mc_p \frac{dT}{dt} = -\varepsilon\sigma AT^4 + Q_{total}.$$

where m is the mass of the component, c_p is the heat, A is the surface area and Q_{total} is the total heat flux from the sun which can be computed for each component. Under this formulation, the analytical solution can be obtained in closed form as:

$$2 \tan^{-1} \gamma T + \log(1 + \gamma T) - \log(1 - \gamma T) = 4\alpha\gamma t + c.$$

where $\gamma = \sqrt[4]{\beta/\alpha}$ and c is the integration constant and specifies the initial temperature $T(0)$. As stated previously, it is in a closed form, for each time step, the root of the closed form equation should be found. The root of equation is found at each time step by bisection algorithm (Chapra, 2006). The analytical solution is used as a reference point to check the accuracy of the time integrator. The comparison between the analytical model and the numerical model is given in Figure 5. As expected, under constant heating, 1-D lumped mass converges to constant temperature, however the numerical error is not visually comparable in Figure 5. The percent error at each time step is also computed as:

$$error_{\%} = 100 \times \left\| \frac{T_{analytical} - T_{numerical}}{T_{analytical}} \right\|.$$

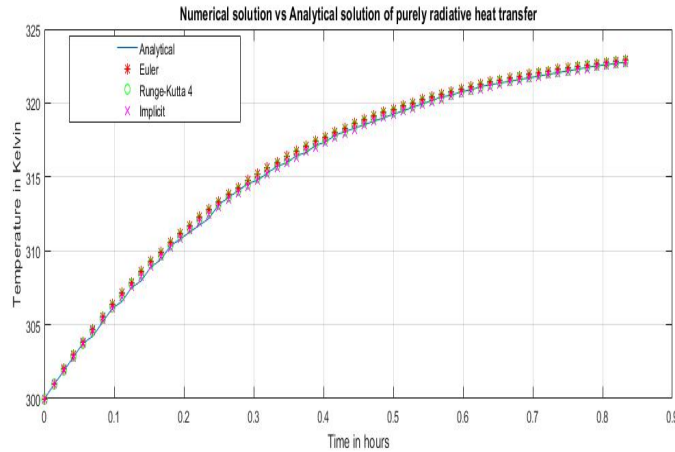


Figure 5: 1-D radiative block getting exposed to the constant heating analytical solution compared with numerical solution via Euler, Runge-Kutta 4 and Implicit time integration.

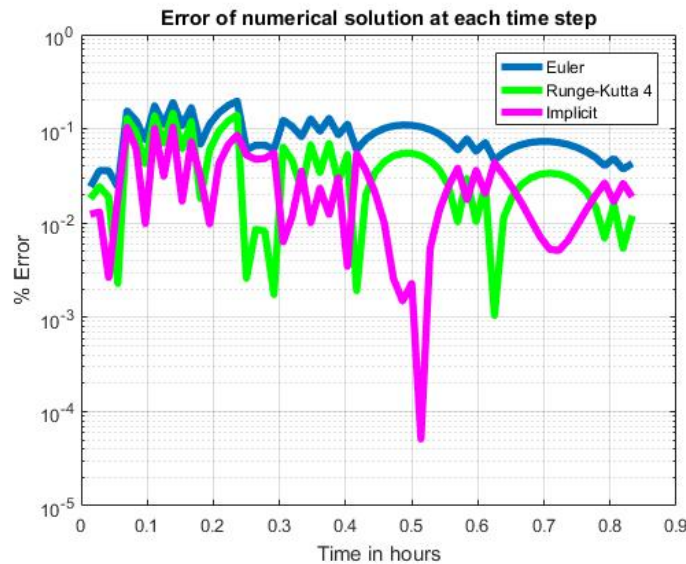


Figure 6: The percent error over time of Euler, Runge-Kutta 4 and Implicit time integrations.

2-D Radiative-Conductive Block

Previously, only radiative problem is analyzed and presented, however the objective of the thermal network model is to analyze both radiative and conductive problem. The radiation condition can also be applied to whole surface based on a problem. Under the radiative condition imposed in the problem analyzed here, the system is supposed to only lose heat from left and right boundaries, therefore temperature is supposed to be lower around these edges. Moreover, even though net heat flux is provided on top and bottom edges, also radiative condition is imposed on these edges too.

In other case, heat fluxes from boundaries are imposed as shown in Figure 7. The heat flux at the boundaries are supposed to mimic the heat flux from sun. Moreover, in this

particular case, the radiation condition is only added to edges. Therefore, the net heat at some time may reach zero if the radiative heat loss reaches same level with the external heating. The number of iterations will increase as the number of nodes increases, however it can be compensated by increasing the time step size Δt . As mentioned earlier, the time integration requires an root finding algorithm in higher dimensions via Newton-Raphson method. It took roughly 50 iterations to get $O(10^{-4})$ error at each time step for $N_x = 10$ which is the number of points in x direction and $N_y = 10$ which is the number of points in y direction in total $N_x \times N_y = 10$ in 2-D problem given here.

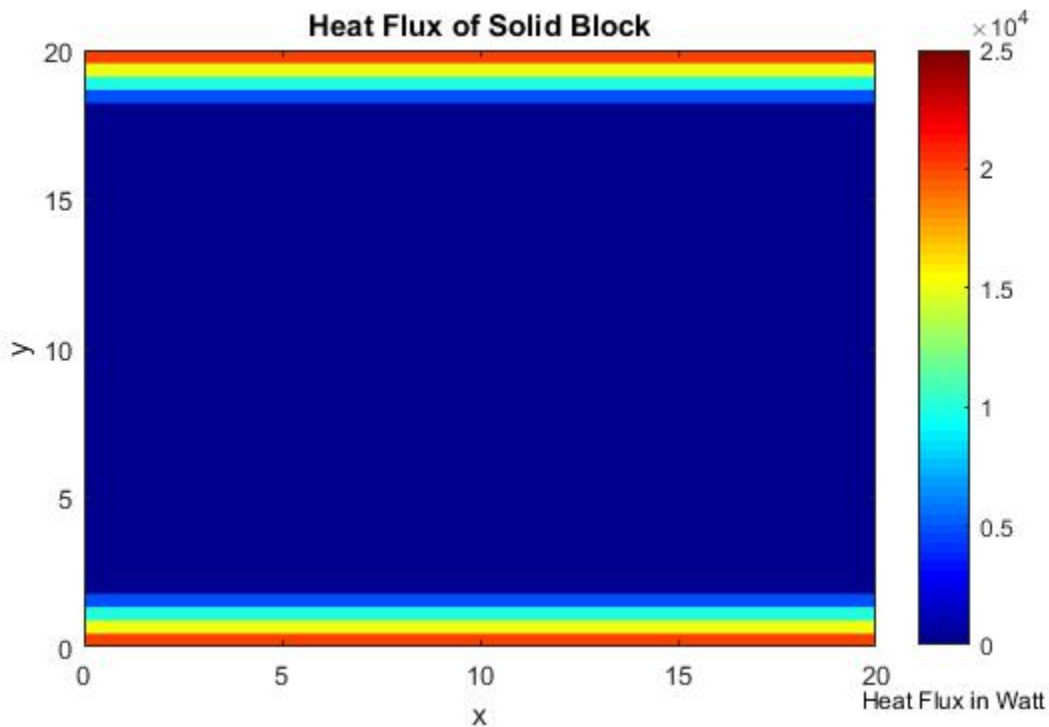


Figure 7: 2-D plate exposed to heating at the top and the bottom boundaries

This type of symmetric heating is also supposed to create symmetric temperature distribution within 2-D block under symmetric radiation from boundaries. An expected temperature distribution is obtained within 2-D block as shown in Figure 8, the temperature is higher on top and bottom boundaries and lower at left and right boundaries.

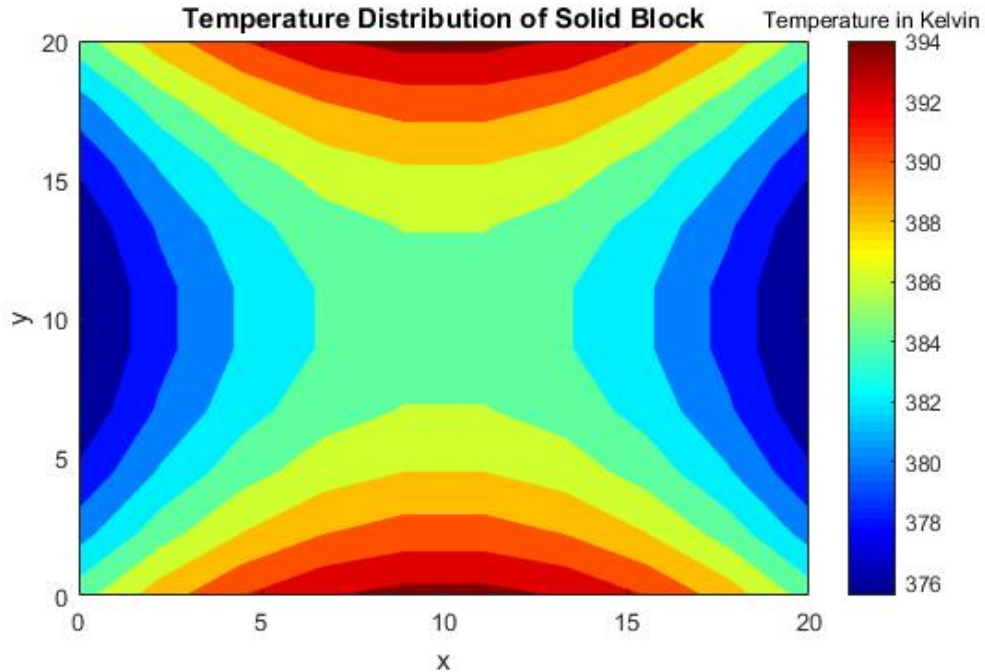


Figure 8: Terminal temperature distribution of 2-D plate exposed to heating at the top and the bottom boundaries and losing heat via radiation from edges.

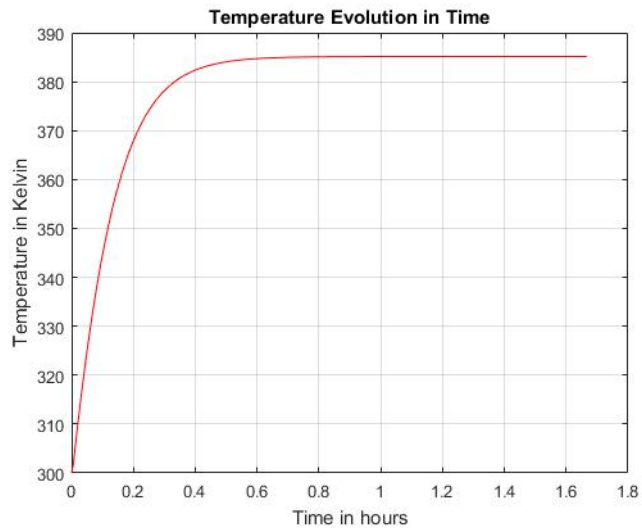


Figure 9: The transient evolution of the average temperature of 2-D plate.

The main physical reason for this transient temperature is that first, the external heating increases the temperature on top and bottom boundaries to a level where these boundaries then the plate starts losing heat via radiation. In addition, the average temperature calculation is also performed. In case of both radiative and conductive case, depending on average radiative heat loss, the average temperature of the system may either increase or

decrease. As shown in Figure 9, the average temperature of the system initially increases then it stays at the constant temperature due to balance between external heat flux and the radiative heat loss.

3-D Discretized Satellite Conduction Radiation problem

In previous analysis, 1-D and 2-D problems are analysed, however it can be readily extended to 3-D problem for any configuration as long as the mass matrix, the conductive matrix and the radiative matrix are imported. The solver treats the problem as higher dimensional time integration problem if these matrices are provided. It also enables to implement models imported from other commercial softwares.

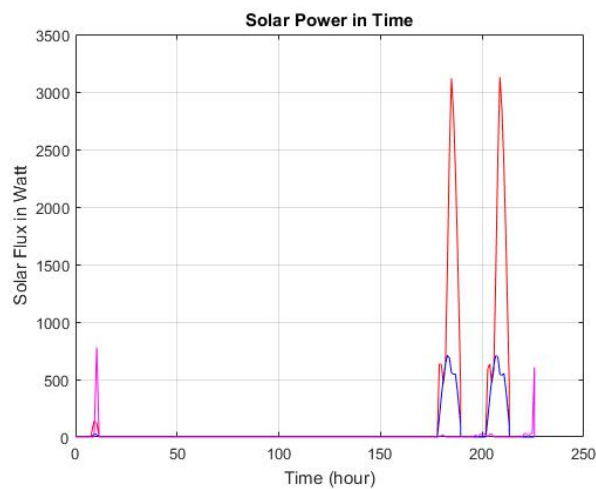


Figure 10: A sample solar flux into one component imported from a commercial software.

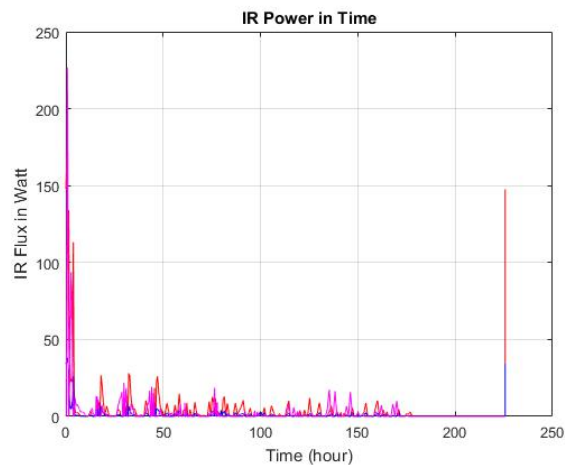


Figure 11: A sample IR flux into one component imported from a commercial software.

The solar, IR and albedo flux given in Figures 11, 12 and 13 are generated with a commercial software to test the solver in 3-D application. However, the solver will be tested

with the experimental results when they are available. Currently, the purpose of the test is to verify the numerical stability of the solver in realistic scenario.

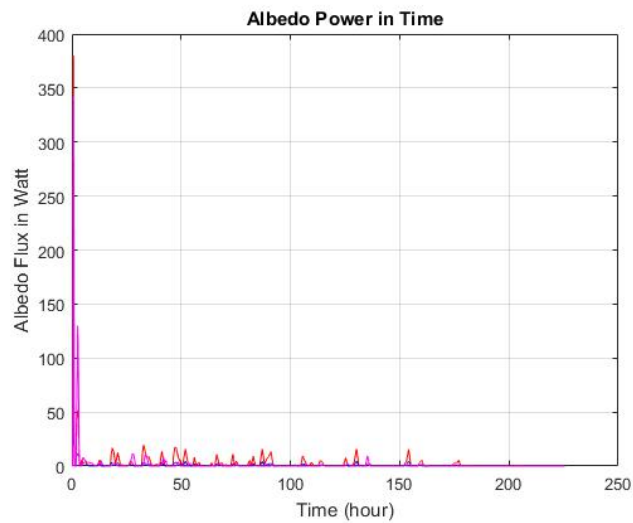


Figure 12: A sample albedo flux into one component imported from a commercial software.

Under these fluxes, the average temperature of the sample satellite at the initial time steps are plotted in Figure 13

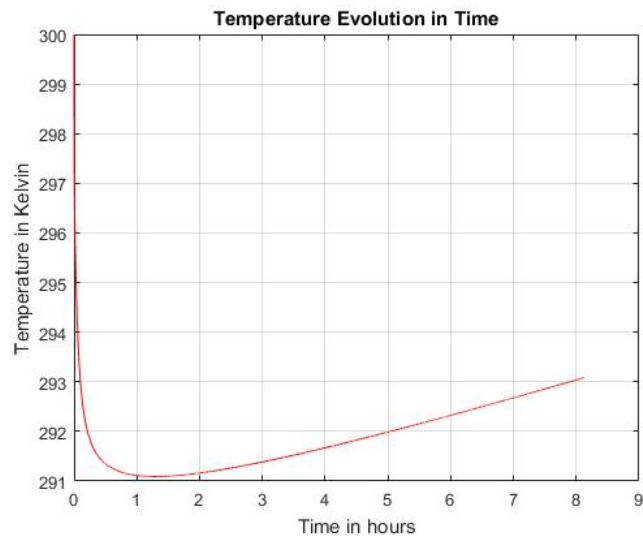


Figure 13: The average temperature of the sample satellite in first 9 hours of heating.

The initial decrease in the average temperature is due to radiative loss to the outer space via radiation. Afterwards, the effect of total heating is felt after first hour then the average temperature steadily increases.

CONCLUSION

In this present study, the objective is to develop a numerical model which can analyse heat transfer problem in satellite. The heat transfer modes in satellite are radiation which enables to transfer heat between components of the satellite and also with outer space. In detail, the heat transfer with outer space includes net heat flux from sun which varies based on satellite's location and radiative heat loss from all surfaces. In addition, conductive heat transfer mode occurs within each component whereas the conduction between components are negligible.

The physical model is one aspect of the problem, another issue to be addressed is to introduce these heat transfer modes to computer. First, the system is written as thermal mass matrix which is multiplied with the time derivative of the system. Moreover, the conduction is discretized and written in terms of conductive connectivity matrix which usually connects the nodes within the same component of the satellite. The radiation is also discretized and given as radiative connectivity matrix which also connects nodes of different components of a satellite. Finally, any external heat load to each node can be given as a right hand side vector which may be a representative of PID controlled heating or cooling mechanism within the satellite.

As for time integration, implicit method is preferred to get more accurate and especially more stable results. The data from the next time step are used to get more accurate approximation of time derivative. Inevitably, it requires implicit time integration which also requires multi-dimension root finding algorithm. In this paper, Newton-Raphson algorithm is preferred. The complexity of the system increases the number of iterations, however the implicit part of integration considerably increases the stability of the algorithm as explained and showed previously which enables to choose larger time step sizes.

All in all, a framework for thermal network analysis for a satellite is presented here. It can be used to control heating and cooling system of a satellite. However, In the current state of the simulator, the measurement data is not incorporated into the simulator, and there is considerable amount of uncertainty associated with the problem analyzed here. However the measurement data can be used to improve the quality of the thermal control by means of non-linear system identification which received considerable attention in other type of non-linear systems (Green, 2015). Similar type of analysis is also done in the calculation of the trajectory of the satellite via Kalman filtering (Noriega, 1992), similar type of Bayesian approach can be taken to get better estimates of associated coefficients used here like mass, conductivity and radiation matrices.

ACKNOWLEDGEMENTS

Authors thank Mr. A. Okan, Mr. E. Mermer, Mr. B. Mıhçak and Mr. Ö. R. Sözbir for enlightening discussions and comments on the early version of the manuscript.

CONTACT

e-mail: anil.aksu@tubitak.gov.tr

NOMENCLATURE, ACRONYMS, ABBREVIATIONS

ε	emissivity
α	absorptivity
ρ	reflectivity
κ	thermal conductivity
σ	Stefan-Boltzmann constant

APPENDIX

1-D Radiation problem analytical solution

1-D transient radiative heat equation can be integrated in time as:

$$\frac{dT}{\alpha - \beta T^4} = dt$$

where $\alpha = Q_{total}/mc_p$ and $\beta = \varepsilon\sigma A/mc_p$. The left hand-side of the equation above can be written in terms of partial fractions as:

$$\frac{1}{2\sqrt{\alpha}(\sqrt{\alpha} + \sqrt{\beta}T^2)} + \frac{1}{4\sqrt[4]{\alpha^3}} \left(\frac{dT}{\sqrt[4]{\alpha} + \sqrt[4]{\beta}T} + \frac{dT}{\sqrt[4]{\alpha} - \sqrt[4]{\beta}T} \right) = dt$$

The expression above can be integrated from both sides, the resultant closed form relation between temperature and time can be given as:

$$2 \tan^{-1} \gamma T + \log(1 + \gamma T) - \log(1 - \gamma T) = 4\alpha\gamma t + c$$

where $\gamma = \sqrt[4]{\beta/\alpha}$ and c is the integration constant and specifies the initial temperature $T(0)$.

REFERENCES

- Badri, M. A. (2018). High performance computation of radiative transfer equation using the finite element method. . *Journal of Computational Physics*, 74–92.
- Bates, J. W. (2001). On Consistent Time-Integration Methods for Radiation Hydrodynamics in the Equilibrium Diffusion Limit : Low-Energy-Density Regime,. *Journal of Computational Physics* , 99–130.
- Capuano, V. (2013). GNSS performances for MEO , GEO and HEO. *International Astronautical Congress*. Beijing, China: the International Astronautical Federation.
- Chapra, S. C. (2006). *Numerical methods for engineers*. Boston: McGraw-Hill Higher Education.
- Chui, C. K. (2009). *Kalman filtering: With real-time applications*. . Springer.
- Çengel, Y. A. (2003). *Heat Transfer: A Practical Approach*. McGraw-Hill.
- Gilmore, D. G. (2002). *Spacecraft Thermal Control Handbook: Fundamental technologies*. AIAA.
- Green, P. L. (2015). Bayesian system identification of a nonlinear dynamica system using a novel variant of Simulated Annealing. . *Mechanical Systems and Signal Processing*, 133–146.
- Guo-dong, X. &. (2009). Run-time Control Design of Micro-Satellite OBC Based on Reconfigurable Architecture. *2009 4th IEEE Conference on Industrial Electronics and Applications*, 2591–2595.
- Kim, J. H. (2017). Study on the reduction method of the satellite thermal mathematical model. . *Advances in Engineering Software*, 37–47.
- Kreng, J. K. (2005). Telemetry, Tracking, and Commanding (TT&C) link considerations for a LEO Sat. *IEEE Aerospace Conference Proceedings*, 1-10.
- Noriega, G. &. (1992). Application of kalman filtering to real-time preprocessing of geophysical data. . *IEEE Transactions on Geoscience and Remote Sensing*, 897–910.
- O. Montenbruck, E. G. (2005). *Satellite Orbits: Models, Methods and Applications*. Springer.
- Ober, C. C. (2004). Studies on the accuracy of time-integration methods for the radiation – diffusion equations. *Journal of Computational Physics*, 743–772.

- Okan, A. (2002). Thermal Analysis Small Satellites. METU Aerospace and Aeronautical Engineering Department, Master's Thesis.
- Pisacane, V. L. (2016). *The Space Environment and Its Effects on Space Systems*. American Institute of Aeronautics & Astronautics.
- Richmond, J. (2010). Adaptive Thermal Modeling Architecture For Small Satellite. . Boston, MA, USA: MIT.
- Sharon, G. (2015). Temperature Cycling and Fatigue in Electronics. , 17. *DFR Solutions* .
- Vujičić, M. R. (2006). Numerical sensitivity and view factor calculation using the Monte Carlo method. . *Proceedings of the Institution of Mechanical Engineers, Part C: Journal of Mechanical Engineering Science*.